A WIND TURBINE BENCHMARK FOR HYBRID SYSTEM ANALYSIS & DESIGN

D.J.Leith[1,2], **W.E.Leithead**[1,2], **O.Mason**[1], **R.Shorten**[1]

[1]*Hamilton Institute, NUI Maynooth, Co. Kildare, Ireland*
[2]*Dept. of Electronic & Electrical Engineering, University of Strathclyde, U.K.*

Abstract
Recent years have witnessed an enormous growth of interest in dynamic systems that are characterised by a mixture of both continuous and discrete dynamics, commonly referred to as hybrid or switching systems. Nevertheless, there is a notable lack of suitable benchmark problems on which to assess and compare competing analysis and design methods. The present paper provides a collection of detailed benchmark design and analysis tasks which, while somewhat simplified in nature, reflect the scale and complexity of the tasks encountered in at least one important application domain, namely wind turbine regulation. *Copyright © 2002 IFAC*

Keywords: Hybrid Systems, Stability Analysis, Control Design Wind Turbines

1. INTRODUCTION

Recent years have witnessed an enormous growth of interest in dynamic systems that are characterised by a mixture of both continuous and discrete dynamics, commonly referred to as hybrid or switching systems. Switched systems arise in a great variety of control applications. Their use to ensure the satisfaction of input and/or output constraints is widespread. Similarly, switched solutions are often used to satisfy changing performance objectives, for example in process. Although gain-scheduled controllers may employ some form of interpolation of the control law between design operating points, simple switching is also used (*e.g.* Leith & Leithead 1996). Switched linear controllers have been proposed as the basis for a variety of adaptive control schemes (e.g. Narendra & Balikrishnan 1994). The potential for improved performance through controller switching is well known. Complementing the design literature, much recent work has focussed on the stability analysis task (see, for example, the review of Liberzon & Morse 1999). Classically, the stability of switched systems is guaranteed for arbitrary switching sequences provided the component systems possess a common Lyapunov function. This property underlies not only the Circle criterion applied to state-space systems but also quadratic stability results (*e.g.* Narendra & Balikrishnan 1994, Shorten & Narendra 1999) and piece-wise quadratic results (*e.g.* Johansson & Rantzer 1998). Stability may also be assured by imposing suitable conditions on the allowable switching sequences. For example, dwell-time ideas and hysteresis switching.. Other types of constraint on the allowable switching sequences are studied by, for example, Branicky 1998. The stability of switched linear systems may also be investigated by examining the local or global topology of trajectories in state-space.

Nevertheless, despite this substantial body of work, there is a notable lack of suitable benchmark problems on which to assess and compare competing analysis and design methods. This situation is exacerbated by the fact that existing analysis methods generally lead, of course, only to sufficiency conditions for stability. An issue of key importance therefore is to determine the nature of the conservativeness incurred and thereby the applications for which a particular method is best suited. However, few results are available in this regard. Related to this issue, many of the examples used in the literature to illustrate analysis methods

involve simplified, very low-order systems which do not necessarily reflect the scale and complexity of system which may be encountered in practice. A similar situation exists in the design literature, where the application of soundly-based methods is often confined to very simplified examples and, while many real applications of switched controllers do indeed exist, these are often designed in an *ad hoc* manner. While the present paper cannot hope to address these issues in itself, the aim here is to provide a collection of detailed benchmark design and analysis tasks which, while still subject to considerable simplification, more accurately reflect the scale and complexity of the tasks encountered in at least one important application domain, namely wind turbine regulation.

The paper is organised as follows. In section 2, a model of the wind turbine dynamics at a level of detail suitable for control analysis and design purposes is described. The performance specification and operating constraints are presented in section 3 and a base-line control design not unlike the type employed within the wind turbine industry is designed and assessed in section 4. In addition to this design task, a number of analysis challenges highlighted by the benchmark example are described in section 5. These challenges highlight a number of aspects, which are of generic interest, of the conservativeness present in standard stability analysis tools.

2. VARIABLE SPEED PITCH-REGULATED WIND TURBINE DYNAMICS

A large-scale 1MW three-bladed grid-connected variable-speed pitch-regulated wind turbine is considered. A block diagram representation of this system is depicted in **Error! Reference source not found.** and the characteristics of the turbine component sub-systems are detailed below (see Leithead & Connor 2000a for detailed, generic derivation and validation of the dynamics).

2.1 Power Train
The combined dynamics of the drive-train and generator are essentially linear and, together, are modelled by

$$\dot{\mathbf{x}}_p = \mathbf{A}_p \mathbf{x}_p + \mathbf{B}_p \mathbf{T}$$

with

$$\mathbf{x}_p = [\Omega_{LD} \quad T_{LS} \quad \Omega_{LS}]^T, \mathbf{T} = [T_{LD} \quad T_{rtr}]^T$$

$$\mathbf{A}_p = \begin{bmatrix} -\gamma_2/I_2 & 1/NI_2 & 0 \\ -\hat{K}_1/N & 0 & \hat{K}_1 \\ (\gamma'/N - \gamma\hat{K}_1/(N^3K_2))/I_1 & -1/I_1 & -(\gamma_1 + \gamma' - \gamma\hat{K}_1/(N^2K_2))/I_1 \end{bmatrix}, \mathbf{B}_p = \begin{bmatrix} -1/I_2 & 0 \\ 0 & 0 \\ 0 & 1/I_1 \end{bmatrix}$$ (2)

where T_{LS} is the torque on the low speed shaft, Ω_{LS} is the speed of the low-speed shaft, Ω_{HS} is the speed of the high-speed shaft, Ω_{LD} is the generator speed, T_{rtr} is the torque generated by the rotor, T_{LD} is the generator reaction torque (set via power electronics). The parameter values are N=58; I_1=1.0295×10^6; I_2=42.82; K_1=1.0106×10^8; K_2=4.85×10^6; γ_1=1.5176×10^4; γ_2=4.5112; γ'= 2.6538×10^5, $\hat{K}_1 = K_1 / \left(1 + \dfrac{K_1}{K_2 N^2}\right)$. (It should be noted that the value of γ_1 embodies the linear component of the damping introduced by aerodynamic effects). The generator speed transfer function associated with the linear dynamics (1) is

$$\Omega_{LD}(s) = \frac{-(0.02335s^2 + 0.00633s + 2.279)T_{LD}(s) + 0.0393T_{rtr}(s)}{s^3 + 0.3764s^2 + 794.9s + 20.57}$$ (3)

2.2 Pitch Actuator
The pitch actuator position is physically constrained to be greater than or equal to zero degrees. By suitably augmenting the plant (see Appendix), the actuator dynamics may be neglected for analysis purposes. For completeness, however, it is noted that these are

$$\dot{\mathbf{x}}_z = \mathbf{A}_a \mathbf{x}_a + \mathbf{B}_a \hat{u}, \quad \hat{p} = \mathbf{C}_a \mathbf{x}_a$$ (4)

where

$$\mathbf{A}_a = \begin{bmatrix} 0 & 1 & 0 \\ -526.62 & -28.57 & -1022.73 \\ v(\hat{p}) & 0 & 0 \end{bmatrix}, \mathbf{B}_a = \begin{bmatrix} 0 \\ 1022.73 \\ 0 \end{bmatrix}, \mathbf{C}_a = [0 \quad 0 \quad 1]_a$$ (5)

and $v(\hat{p}) = \begin{cases} 1 & \hat{p} > 0 \\ 0 & \hat{p} \leq 0 \end{cases}$ embodies the position constraint.

2.3 Aerodynamics
By suitably augmenting the plant, the aerodynamic torque, T_{rtr}, generated by the rotor may be approximately modelled as

$$T_{rtr} = K_V V^2 - K_p \Delta(p, \Omega_{LS}) p$$ (6)

where is the effective blade pitch angle, Ω_{LS} the rotor speed, V the effective wind speed, $\Delta(p, \Omega_{LS})$ is an unknown gain (embodying uncertainty as to the aerodynamic characteristics) with nominal value of unity, K_p=29500.0 and K_V=3200.0.

2.4 Wind Disturbance
The effective wind speed over the rotor disk is modelled, for mean wind speeds V_{mean} by the linear stochastic equations

$$\begin{bmatrix} \dot{V}_{point} \\ \dot{a}_{x_1} \\ \dot{a}_{x_2} \end{bmatrix} = \begin{bmatrix} -a_w(V_{mean}) & 0 & 0 \\ \dfrac{\tau_1}{\tau_2\tau_3} & 0 & 1 \\ \dfrac{\tau_2\tau_3 - \tau_1(\tau_2 + \tau_3)}{\tau_2^2\tau_3^2} & \dfrac{1}{\tau_2\tau_3} & \dfrac{(\tau_2 + \tau_3)}{\tau_2\tau_3} \end{bmatrix} \begin{bmatrix} V_{point} \\ a_{x_1} \\ a_{x_2} \end{bmatrix} + \begin{bmatrix} b_w(V_{mean}) \\ 0 \\ 0 \end{bmatrix} \eta, V = [0 \quad 1 \quad 0] \begin{bmatrix} V_{point} \\ a_{x_1} \\ a_{x_2} \end{bmatrix}$$ (7)

where η is Gaussian white noise with zero mean and unity variance, values for a_w and b_w (capturing the increase in wind turbulence experienced with increasing mean wind speed) are given in Table 1, $\tau_1 = \beta/\sqrt{2}, \tau_2 = \tau_1\sqrt{a}, \tau_3 = \beta/\sqrt{a}$ (1) and $\beta = 33.8/V_{mean}, a = 0.55$ with V_{mean} a constant denoting the mean effective wind speed (m/s).

V_{mean} (m/s)	a_w	b_w
8	0.060	0.74
10	0.062	0.77
16	0.092	1.37
22	0.125	1.63

Table 1 Filter parameters for wind disturbance model.

3. A BENCHMARK DESIGN TASK: CONTROL REQUIREMENTS
The overall objective of the controller is to maximise energy production while working within actuator operational limits and minimising the peak loads, and associated fatigue damage, on the turbine structure and drive train. This is a disturbance rejection task.

3.1 Measured Variables
Measurements are available of (i) the instantaneous power P (*i.e.* the product $T_{LD}\Omega_{LD}$) and (ii) the generator

speed Ω_{LD}. The sensor dynamics can be assumed negligible, as is measurement noise. Note that the effective wind speed, V, *cannot* be measured.

3.2 Manipulated Variables
The controller is able to adjust (i) the blade pitch angle and (ii) the generator reaction torque, T_{LD}.

3.3 Physical Constraints
Controller activity is constrained by two main operational factors. Firstly, the controller is required to operate within the constraints of the available actuator. In addition to the constraints that the blade angle is non-negative, the machine considered here employs a hydraulic pitch actuator for which the relevant measure of actuator activity is the velocity of the blade pitch angle. The standard deviation of the pitch angle velocity (filtered by the actuator dynamics (4)) reflects the actuator activity over the medium and long term and is required to remain below the curve 0.4V-1.8 deg/s over the operating range of mean wind speeds up to 24 m/s. Secondly, in order to avoid exciting structural resonances and to remain within design loadings, the turbine is not to be continuously operated (*i.e.* in steady state) at rotor speeds above 2.72 rads/sec. In addition to this continuous operating limit, the rotor speed transients induced by wind turbulence must remain strictly less than 3.4 rads/sec under the normal range of operating conditions. The former limit is denoted $\Omega_{LS}^{max\,cont}$ and the latter Ω_{LS}^{max}. The generator reaction torque, T_{LD}, must be positive (to avoid "motoring") and the generator is not to be operated continuously (*i.e.* in steady state) above a level, P_{rated}, of 1MW.

3.4 Robustness
The uncertainty in the plant dynamics is primarily associated with the rotor aerodynamics. In addition to the use of a relatively crude aerodynamic model for control design purposes, the rotor aerodynamics typically exhibit considerable variation during normal operation (associated with, in particular, the accumulation of environmental deposits on the blade surfaces). The closed-loop system is therefore required to remain stable for arbitrary time variations in the uncertain gain Δ in the interval [0.5,2].

3.5 Operational Requirement
The overall objective of the controller is to maximise energy production while working within the operational limits of the turbine and minimising the peak loadings experienced. While the wind is highly stochastic, initial insight into this requirement can be gained by considering the situation when the wind is steady and the turbine is in equilibrium. Three operating modes can be identified.

1. Energy capture limited by available wind energy
2. Energy capture limited by rotor speed constraints
3. Energy capture limited by generator rating

Performance Assessment
Performance is measured as follows (the approach adopted is semi-empirical in view of the complex, stochastic nature of the wind disturbance; see Leithead & Connor 2000b). Time histories of the controlled system are collected for turbulent wind conditions with mean wind speeds $V_{mean} \in \{6,8,10,12,14,16,18,22,24\}$ m/s. The time histories are each of 600 seconds duration (after discarding the initial 20 seconds to allow the system to settle down) and are partitioned into 10 second intervals. The mean wind speed, mean power, mean generator torque, peak power, maximum rotor speed, minimum generator torque and standard deviation of pitch actuator velocity are determined for each interval. This interval data is sorted into 1 m/s wide bins according to mean wind speed. Let V_i denote the centre wind speed of the ith bin. The average of the mean power data in the ith bin is a measure of energy capture at wind speed V_i. Let σ_i denote the standard deviation of the peak power data in the ith bin and μ_i denote the average of the peak power data in the ith bin. Then $\mu_i + 3\sigma_i$ is a measure of the peak load experienced by the wind turbine at wind speed V_i. Energy capture is to be maximised and peak loads minimised, subject to operating constraints. With regard to the latter, similar calculations for the maximum rotor speed data, minimum generator torque data and pitch actuator velocity data provides an upper bound on Ω_{LS} (required to be less than Ω_{LS}^{max}), a lower bound on T_{LD} (required to be positive) and an upper bound on pitch actuator velocity. A further, deterministic, extreme gust is employed to confirm the ability of the controller to maintain operation within the allowed rotor speed limits. This gust is a pulse with an initial wind speed of 22 m/s, falling to 12 m/s for 10 seconds and then returning to 22 m/s.

4. BASELINE DESIGN: CLASSICAL CONTROLLER
While the turbine dynamics themselves are essentially linear, owing to the various operating constraints it is evident that the performance requirement cannot be met by a single linear controller. Reflecting the natural decomposition of the turbine operation into different regimes, a divide and conquer design approach similar to that presently employed in a commercial context is to design an individual controller for each mode of operation and then integrate these to obtain a full envelope controller.

4.1 Operating Mode 1
Under nominal steady state conditions, the maximum power is generated when $T_{LD} = K_V V^2 / 2N$. Unfortunately, as the effective wind speed V is unmeasurable, direct regulation of T_{LD} to meet this equality is impossible. Instead, an indirect approach must be used. In steady conditions generating maximum power, the generator speed is $\Omega_{LD} = NK_V V^2 / 2(\gamma_1 + N^2\gamma_2)$. That is, $K_v V^2 = 2(\gamma_1 + N^2\gamma_2)\Omega_{LD} / N$. Consider, therefore, the control law

$$T_{LD} = C_{LD} \frac{(\gamma_1 + N^2\gamma_2)}{N^2} \Omega_{LD} \qquad (8)$$

where $C_{LD} = \dfrac{1}{0.05s + 1}$ $\qquad (9)$

provides additional roll-off to compensate for the resonance in the turbine drive-train.

4.2 Operating Mode 2

The controller is configured to regulate rotor speed at a constant value by adjusting the generator reaction torque while maintaining the blade pitch angle at zero. Using classical loop-shaping techniques, the controller transfer function is designed to incorporate integral action to ensure rejection of changes in mean wind speed. The controller designed is

$$T_{LD} = C_1\left(N\Omega_{LS}^{max\,cont} - \Omega_{LD}\right) + C_{LD}\frac{(\gamma_1 + N^2\gamma_2)}{N^2}\Omega_{LD} \quad (10)$$

where C_1 and C_{LD} denote linear dynamics with transfer functions

$$C_1 = \frac{1200(5s+1)}{s(s^2+4s+14)(0.05s+1)} \quad (11)$$

Observe that, with the aim of simplifying the overall design, the mode 2 controller (10) is obtained by suitably augmenting the existing mode 1 controller, (8). The gain margin is 9.67 dB, the phase margin is 56.51° and the cross-over frequency is 1.30 rad/s.

4.3 Operating Mode 3
Neglecting, for the moment, the high frequency drive-train resonance, the plant dynamics (1) may be simplified to

$$\dot{\Omega}_{LD} = \frac{NT_{atr} - N^2T_{LD} - \gamma_1\Omega_{LD}}{I_1} = \frac{-NK_p p - N^2 T_{LD} - \gamma_1\Omega_{LD}}{I_1} + \frac{NK_v}{I_1}V^2 \quad (12)$$

Evidently, the aerodynamic torque and generator torque are matched in the sense that they enter the equation in the same manner, albeit with a gain difference of N. Hence, despite the physical structure of the system being quite different in modes 2 and 3 (in mode 2 control action applied via the generator torque alone, while in mode 3 the system is configured as MIMO with control action applied via both the pitch angle and generator torque), in terms of the plant dynamic characteristics these modes are closely related.

   In mode 3 the generator torque is held constant and the blade pitch angle adjusted to regulate the rotor speed at the continuous operating value $\Omega_{LS}^{max\,cont}$. Using classical loop-shaping techniques, the controller is designed as

$$u = \frac{N}{K_p}C_2\left(N\Omega_{LS}^{max\,cont} - \Omega_{LD}\right) + \frac{(\gamma_1 + N^2\gamma_2)}{N^2}\Omega_{LD} \quad (13)$$

where C_2 denotes linear dynamics with transfer function

$$C_2 = \frac{1200(5s+1)}{s(s^2+4s+14)} \quad (14)$$

Observe that, at least at low frequencies, the controller transfer function is closely related to that employed in mode 2, reflecting the similarity in plant dynamics in modes 2 and 3 noted previously. The gain margin is 9.84 dB, the phase margin is 59.63° and the cross-over frequency is 1.33 rad/s.

4.4 Full Envelope Controller
It remains to integrate the separate mode 1, 2 and 3 controllers to produce a full-envelope controller implementation. Firstly, it is noted that the mode 2 and 3 controllers are designed to directly augment the mode 1 controller, thereby simplifying implementation. Secondly, the mode 2 and 3 controllers possess similar low frequency dynamics. The latter can be made explicit by partitioning the mode 2 and 3 controller transfer functions as

$$C_1 = C_{LD}C_{low}, \quad C_2 = C_{low} \quad (15)$$

where

$$C_{low} = \frac{1200(5s+1)}{s(s^2+4s+14)}, \quad C_{LD} = \frac{1}{(0.05s+1)} \quad (16)$$

During mode 1 operation, the integrator in C_{low} can "wind up" resulting in excessive transients following a transition from mode 1 to mode 2 operation. Transients may also be associated with the other low frequency dynamics elements of C_{low}. Following Leith & Leithead (1997), and similarly to a number of popular anti-wind up approaches, this issue is addressed here by partitioning C_{low} as $C_{low} = C_o C_i$ where

$$C_i = -15.625\frac{(5s+1)}{s(s^2+4s+14)}, \quad C_o = 76.8 \quad (17)$$

and enclosing the dynamics C_i within a minor feedback loop during mode 1 operation. The partitioning into C_o and C_i is selected such that the bandwidth of the minor loop is similar to that of the closed-loop system during mode 2/3 operation. Switching from mode 2 to mode 3 operation is based on the generator reaction torque. The resulting full envelope controller implementation is shown in Figure 2. Observe that the switches within the controller are formulated as continuous (but non-differentiable) nonlinear functions of the switch input. Hence, the admissible switching sequences are immediately evident from the block diagram. The constant T_{ref} introduced in the block diagram is defined by

$$T_{ref} = P_{rated}/N\,\Omega_{LS}^{max\,cont} \quad (18)$$

That is, T_{ref} is the generator torque at which rated power is developed when operating at rated speed. This is used within the controller in a straightforward manner as a threshold on internal signals to determine the required mode of operation.

Remark The following state-space realisations are employed.
$$C_{LD}: \quad \dot{\mathbf{x}}_{LD} = \mathbf{A}_{LD}\mathbf{x}_{LD} + \mathbf{B}_{LD}T_1, \quad T_{LD} = \mathbf{C}_{LD}\mathbf{x}_{LD} \quad (19)$$
$$C_iC_o: \quad \dot{\mathbf{x}}_{low} = \mathbf{A}_{low}\mathbf{x}_{low} + \mathbf{B}_{low}\left(\left(N\Omega_{LS}^{max\,cont} - \Omega_{LD}\right) + B_o T_1\right), \quad T_2 = \mathbf{C}_{low}\mathbf{x}_{low}$$
where

$$\left[\begin{array}{c|c}\mathbf{A}_{LD} & \mathbf{B}_{LD} \\ \hline \mathbf{C}_{LD} & \mathbf{D}_{LD}\end{array}\right] = \left[\begin{array}{c|c}-20 & 4 \\ \hline 5 & 0\end{array}\right], \quad \left[\begin{array}{c|c}\mathbf{A}_{low} & \mathbf{B}_{low} \\ \hline \mathbf{C}_{low} & \mathbf{D}_{low}\end{array}\right] = \left[\begin{array}{ccc|c}-40 & -35 & 0 & -31.25 \\ 40 & 0 & 0 & 0 \\ 25 & 0.125 & 0 & 0 \\ \hline [0\ 0\ 1] & 0\end{array}\right], \quad B_o = 0.0130$$

$$(20)$$

4.5 Performance
Performance plots for the baseline controller are omitted owing to space considerations but are available at www.hamilton.may.ie, together with a Simulink model of the plant and controller Needless to say, the controller fully meets the performance specification.

5. ANALYSIS CHALLENGES
The baseline controller design immediately creates a number of analysis tasks. While analysis of the robust stability and performance of the full-envelope closed-loop system is required, the local pair-wise analysis of the operating modes nominal stability presents a task of sufficient difficulty for present purposes.

5.1 Stability of Mode 1/2 Operation
During operation encompassing modes 1 and 2, the closed-loop dynamics (neglecting the additive wind

disturbance and the constant reference inputs to the controller) are

$$\dot{\mathbf{x}} = \mathbf{A}_i \mathbf{x}, \quad i \in \{1,2\} \tag{21}$$

$$\mathbf{x} = \begin{bmatrix} \mathbf{x}_p & \mathbf{x}_{aw} & \mathbf{x}_{LD} \end{bmatrix}^T, \mathbf{A}_1 = \begin{bmatrix} \mathbf{A}_p & 0 & \mathbf{B}_{p1}\mathbf{C}_{LD} \\ -\mathbf{B}_{aw}\mathbf{C}_p & \mathbf{A}_{aw}+\mathbf{B}_{aw}\mathbf{B}_p\mathbf{C}_{low} & 0 \\ \mathbf{B}_{LD}\frac{(\gamma_1+N^2\gamma_2)}{N^2}\mathbf{C}_p & 0 & \mathbf{A}_{LD} \end{bmatrix} \mathbf{A}_2 = \begin{bmatrix} \mathbf{A}_p & 0 & \mathbf{B}_{p1}\mathbf{C}_{LD} \\ -\mathbf{B}_{aw}\mathbf{C}_p & \mathbf{A}_{aw} & 0 \\ \mathbf{B}_{LD}\frac{(\gamma_1+N^2\gamma_2)}{N^2}\mathbf{C}_p & \mathbf{B}_{LD}\mathbf{C}_{low} & \mathbf{A}_{LD} \end{bmatrix}$$

$$\tag{22}$$

where $\mathbf{B}_{p1}$ denotes the first column of $\mathbf{B}_p$, $\mathbf{C}_p = [1\ 0\ 0]$.

One standard approach to stability analysis of a switched system of the form (21) is to search for a common quadratic Lyapunov function (CQLF), $\mathbf{x}^T\mathbf{P}\mathbf{x}$. That is, for a matrix $\mathbf{P}$ such that

$$\mathbf{P} > 0, \quad \mathbf{A}_1^T\mathbf{P}+\mathbf{P}\mathbf{A}_1 < 0, \quad \mathbf{A}_2^T\mathbf{P}+\mathbf{P}\mathbf{A}_2 < 0 \tag{23}$$

The existence of such a matrix guarantees the exponential stability of (21) for all switching sequences (*e.g.* see Liberzon & Morse 1999, Shorten & Narendra 1998 and references therein). However, a direct search for a matrix $\mathbf{P}$ satisfying the inequalities (23) performed using the LMI toolbox in MATLAB fails to establish the existence of a CQLF for the system (21). Indeed, it can be confirmed without resort to LMI methods that no CQLF exists for this system (details omitted here due to space considerations). It is easy to confirm that the Circle criterion also fails to establish the stability of (21). It is noted that this is unsurprising since the Circle criterion is closely related to CQLF methods but is nevertheless included here for completeness.

While the forgoing analysis considers quadratic Lyapunov functions, LMI based analysis may be extended to encompass searching for the existence of a class of piecewise-quadratic Lyapunov functions (Johansson & Rantzer 1998). The state-space is divided into two regions or cells, with mode 1 effective in cell 1 ($x_6 < 0$) and mode 2 effective in cell 2 ($x_6 \geq 0$). To establish stability via piecewise methods, a Lyapunov function of the form

$$V(x) = \begin{cases} \mathbf{x}^T\mathbf{P}_1\mathbf{x} & \text{in cell 1} \\ \mathbf{x}^T\mathbf{P}_2\mathbf{x} & \text{in cell 2} \end{cases} \tag{12}$$

is sought, where the matrices $\mathbf{P}_i$ are parameterised so as to ensure that the function is continuous across the boundaries between the cells. Namely, following Johansson & Rantzer (1998) the matrices $\mathbf{P}_i$ are parameterised as $\mathbf{P}_i = \mathbf{F}_i^T\mathbf{T}\mathbf{F}_i$, i=1,2 where the matrix $\mathbf{T}$ is to be determined and $\mathbf{F}_1\mathbf{x} = \mathbf{F}_2\mathbf{x}$ on the shared cell boundary. Note that these matrices are not uniquely determined by the partition. This formulation relaxes the requirement of a common quadratic Lyapunov function in two ways. Firstly, we do not require a single positive definite matrix $\mathbf{P}$ to simultaneously satisfy $\mathbf{A}_i^T\mathbf{P}+\mathbf{P}\mathbf{A}_i < \mathbf{0}$ for each i. Secondly, when implementing the search for such a function as a system of LMIs, $\mathbf{x}^T(\mathbf{A}_i^T\mathbf{P}_i+\mathbf{P}_i\mathbf{A}_i)\mathbf{x}$ is not required to be negative for all non-zero $\mathbf{x}$ but only for those $\mathbf{x}$ in the cell i where the dynamics are given by the system matrix $\mathbf{A}_i$. The problem of finding a PQLF for the system can be formulated as a feasibility problem for a system of LMIs (Johansson & Rantzer 1998). The PWLTOOL package (Hedlund & Johansson, 1999) for analysis of piecewise linear systems was used to test for the existence of a PQLF. Unfortunately, PWLF

analysis also fails to establish the stability of the system.

Less conservative results can be obtained using harmonic balance techniques at the price of reduced rigour. The describing function of a real, memoryless switch is a real gain in the interval [0,1]. Harmonic balance analysis indicates stability of the switched system. This result is supported by extensive nonlinear simulations.

In view of the foregoing results, the challenge is evidently to derive stability analysis methods capable of providing tight, yet soundly-based, results for the type of system considered here. The lack of non-conservative stability analysis methods is surely one of the major outstanding issues in the control field today. Of particular interest in the present example is the close link between switching system methods and anti-windup techniques which it exemplifies. The existence of a relationship between anti-windup and bumpless transfer methods is often noted at an intuitive level but it is less often discussed in the context of the rigorous stability analysis of switched systems. The key role of the conditioning loop within the controller here in avoiding prolonged transient excursions following switching is readily verified by simulation testing (see also the examples studied in Leith & Leithead (1997) in the context of constant-speed wind turbines) yet despite much work in the switched system and anti-windup fields current techniques for the design of such loops remain largely *ad hoc* in nature.

5.2 Stability of Mode 2/3 Operation
Assume, for the moment, that the filter C_{LD} has sufficiently fast dynamics that the switch within the controller can be moved to the input of C_{LD}. Under these conditions, the switches in the pitch angle and generator torque channels of the controller operate synchronously. It follows that the closed-loop dynamics (neglecting the additive wind disturbance and the constant reference inputs to the controller) are then

$$\dot{\mathbf{x}} = \mathbf{A}_i\mathbf{x}, \quad i \in \{2,3\}$$

with

$$\mathbf{A}_3 = \begin{bmatrix} \mathbf{A}_p-\mathbf{B}_{p2}\dfrac{(\gamma_1+N^2\gamma_2)}{N}\mathbf{C}_p & -\mathbf{B}_{p2}N\mathbf{C}_{low} & 0 \\ -\mathbf{B}_{low}\mathbf{C}_p & \mathbf{A}_{low} & 0 \\ \mathbf{B}_{LD}\dfrac{(\gamma_1+N^2\gamma_2)}{N^2}\mathbf{C}_p & \mathbf{B}_{LD}\mathbf{C}_{low} & \mathbf{A}_{LD} \end{bmatrix} \tag{25}$$

where $\mathbf{B}_{p2}$ denotes the second column of $\mathbf{B}_p$. As in section 5.1, the stability of this system may be analysed using CQLF techniques. A direct search performed using the LMI toolbox in MATLAB, successfully establishes the existence of a CQLF and thereby the exponential stability of the system.

The validity of the foregoing synchronicity assumption is, however, very debatable. Consider therefore relaxing this assumption that the torque switch may be moved to the input of the C_{LD} dynamics. The input to the torque channel switch is simply the input to the pitch switch filtered by C_{LD}. The C_{LD} dynamics are fast compared to the bandwidth of the closed-loop system and thus, while the switches in the pitch and torque channels are asynchronous, the asynchronicity can only exist transiently. Nevertheless, this change has a profound impact on the stability analysis. For CQLF-type stability analysis, the closed-loop system is now conventionally modelled as

switching between four possible system matrices rather than two. The extra two matrices correspond to transient situations whereby the pitch and torque switches are either simultaneously active or simultaneously inactive. Equivalently, the closed-loop can be modelled as

$$\dot{\mathbf{x}} = \mathbf{Ax} + \mathbf{BK(y)y}, \quad \mathbf{y} = \mathbf{Cx} + \mathbf{Dr} \tag{26}$$

where

$$\mathbf{A} = \begin{bmatrix} \mathbf{A}_p & 0 & 0 \\ -\mathbf{B}_{tw}\mathbf{C}_p & \mathbf{A}_{tw} & 0 \\ \mathbf{B}_{LD}\frac{(\gamma_1+N^2\gamma_2)}{N^2}\mathbf{C}_p & \mathbf{B}_{LD}\mathbf{C}_{tw} & \mathbf{A}_{LD} \end{bmatrix}, \mathbf{B} = \begin{bmatrix} \mathbf{B}_p & -\mathbf{B}_p\mathbf{K}_i \end{bmatrix}, \mathbf{C} = \begin{bmatrix} 0 & 0 & \mathbf{C}_{LD} \\ \frac{(\gamma_1+N^2\gamma_2)}{N^2}\mathbf{C}_p & \frac{N\mathbf{C}_{tw}}{K_i} & 0 \end{bmatrix}, \mathbf{D} = 0, \mathbf{K(y)} \in \left\{ \begin{bmatrix}1&0\\0&0\end{bmatrix} \begin{bmatrix}0&0\\0&1\end{bmatrix} \begin{bmatrix}0&0\\0&0\end{bmatrix} \begin{bmatrix}1&0\\0&1\end{bmatrix} \right\}$$

The stability of (26) can be assessed using direct CQLF search techniques and also via related small gain techniques such as the Circle criterion (*e.g.* see Khalil 1992). However, owing to the integral action within the controller, the closed-loop system is not exponentially stable for the case where both switches are simultaneously inactive and the system is effectively operating open-loop. While this situation exists only as a transient condition in the actual system, this information is not embodied in the representation (26) used for stability analysis purposes. The lack of information in (26) regarding this aspect of the switching behaviour means that there exist switching sequences in (26), which are not feasible in the actual system. In particular, there exist switching sequences for which (26) is not exponentially stable. Hence, no method based on this representation can establish the stability of the actual system. The challenge, therefore, is to develop analysis techniques which, by taking greater account of the admissible switching sequences, are capable of establishing the stability of the mode 2/3 regime of operation without the need for unrealistic assumptions such as that of synchronicity used above. It is noted that the manner in which the system in Figure 2 is formulated, whereby the switches are each SISO nonlinear functions of their input, is strongly structured yet rather general, thus providing an interesting class of systems for which the potential exists for developing analysis methods which are of wide application yet not unduly conservative.

REFERENCES

Branicky,M.S., 1998, Multiple Lyapunov Functions and Other Analysis Tools for Switched and Hybrid Systems. *IEEE Trans. Aut. Control*, **43**, 475-482.

Johansson, M., Rantzer, A., 1998, Computation of Piecewise Quadratic Lyapunov Functions for Hybrid Systems. *IEEE Trans Aut. Cont.*,**43,**555-559

Leith, D.J., Leithead, W.E. (1996) Performance Enhancement of Wind Turbine Power Regulation by Switched Linear Control. *Int. J. Contro*l, **65**, 555-572; (1997) Implementation of Wind Turbine Controller*s*. *Int.J.Contro*l,**66**,349-380; (1999) Global Gain-Scheduling Control for Variable Speed Wind Turbine*s*. *Proc. Europ. Wind Energy Conf.*.

Leithead,W.E., Connor,B. (2000a) Control of Variable Speed Wind Turbines: Dynamic Models. *Int. J. Contr.*, **73**, 1173-1188 (2000b) Control of Variable Speed Wind Turbines: Design Task. *Int. J. Contr.*, **73**, 1189-1212.

Liberzon,D., Morse, A.S., 1999, Basic Problems in Stability and Design of Switched Systems. *IEEE Control Systems Magazin*e, 59-70.

Narendra,K.S., Balikrishnan,J. (1994a) Improving Transient Response of Adaptive Control Systems Using Multiple Models and Switching. *IEEE Trans. Aut. Control*, **39**, 1861-1866; (1994b) A Common Lyapunov Function for Stable LTI Systems with Commuting A-Matrices. *IEEE Trans. Aut. Control*, **39**, 2469-2471..

Shorten,R.N., Narendra,K.S., 1998, Necessary and Sufficient Conditions for the Existence of a Common Quadratic Lyapunov Function for Two Stable Second Order Linear Time-Invariant Systems. *Proc Am. Control Conf.*, San Diego.
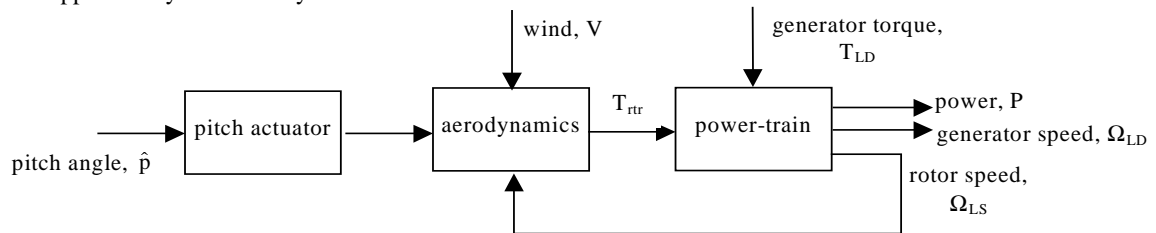
Figure 1 Block diagram representation of wind turbine

Key: denotes an element which only passes positive signals.

denotes an element which only passes negative signals.